Journal of Nuclear Materials 389 (2009) 23–28

Contents lists available at ScienceDirect

Journal of Nuclear Materials

journal homepage: www.elsevier.com/locate/jnucmat

Thermochemical and thermophysical properties of minor actinide compounds

Kazuo Minato *, Masahide Takano, Haruyoshi Otobe, Tsuyoshi Nishi, Mitsuo Akabori, Yasuo Arai

Nuclear Science and Engineering Directorate, Japan Atomic Energy Agency, Tokai-mura, Ibaraki-ken 319-1195, Japan

A B S T R A C T

Burning or transmutation of minor actinides (MA: Np, Am, Cm) that are classified as the high-level radioactive waste in the current nuclear fuel cycle is an option for the advanced nuclear fuel cycle. Although the thermochemical and thermophysical properties of minor actinide compounds are essential for the design of MA-bearing fuels and analysis of their behavior, the experimental data on minor actinide compounds are limited. To support the research and development of the MA-bearing fuels, the property measurements were carried out on minor actinide nitrides and oxides. The lattice parameters and their thermal expansions were measured by high-temperature X-ray diffractometry. The specific heat capacities were measured by drop calorimetry and the thermal diffusivities by laser-flash method. The thermal conductivities were determined by the specific heat capacities, thermal diffusivities and densities. The oxygen potentials were measured by electromotive force method.

1. Introduction

Minor actinides (MA: Np, Am, Cm) are produced from fuel materials of uranium and plutonium in the nuclear reactors through neutron captures and decays, and those in the spent fuels are classified as the high-level radioactive waste in the current nuclear fuel cycle. To reduce the radiotoxicity and heat generation of the high-level radioactive waste and to use the repository efficiently, burning or transmutation of minor actinides as well as plutonium into short-lived or stable elements is an option for the future nuclear fuel cycle. Many concepts have been proposed and studied on MA-bearing fuels together with transmutation systems including critical reactors and accelerator-driven systems (ADS) with sub-critical cores.

Among various fuel types, the nitride fuel has good potentials for the transmutation of minor actinides with ADS [1]. The melting point of the nitride fuel is higher than that of the metal fuel and comparable to that of the oxide fuel. For the thermal conductivity, the nitride fuel is higher than the oxide fuel and comparable to the metal fuel. The nitride fuel supports a hard neutron spectrum needed for fissions of the minor actinides. The actinide mononitrides would form solid solution, which could accommodate a wide range of the combination and composition of actinides.

The oxide fuel has been used in the current power reactors with accumulating much achievement and experience in fabrication and irradiation. The MA-bearing oxide fuel may be put in the first place to practical use for the transmutation of minor actinides. The composite type fuels of CERCER and CERMET have been studied for the transmutation of minor actinides, where U-free oxides are dispersed in the inert matrix phases of MgO and Mo, respectively [2,3].

Although the thermochemical and thermophysical properties of minor actinide compounds are essential for the design of MA-bearing fuels and analysis of their behavior, the data on minor actinide compounds are limited. The properties of actinide compounds of nitrides and oxides have been reviewed [4–6], where it was recognized that the experimental data on americium and curium compounds were almost lacking and that some data on neptunium compounds were available in literature though they were insufficient.

The handling of americium and curium compounds is more difficult than that of uranium compounds due to their γ- and α-rays and neutron emissions as well as their hygroscopic nature. To support the research and development of the MA-bearing fuels, the authors installed new facilities with a purified argon gas atmosphere for property measurements of minor actinide compounds [7]. This paper gives an overview of the recent results of the property measurements of minor actinide nitrides and oxides.

2. Properties of actinide nitrides

2.1. Miscibility of actinide nitrides

Actinide nitrides were synthesized from the oxides by the carbothermic reduction method, where the actinide oxides mixed with carbon were heated in flowing N_2 gas to form the nitrides followed by heating in N_2–H_2 mixed gas to remove the residual carbon. Preparation of actinide nitrides of AmN and (Cm,Pu)N has been reported [8,9], besides UN, NpN, PuN, (U,Pu)N, (U,Np)N and

* Corresponding author. Tel.: +81 29 282 5382; fax: +81 29 282 5922.
E-mail address: minato.kazuo@jaea.go.jp (K. Minato).

0022-3115/$ - see front matter © 2009 Elsevier B.V. All rights reserved.
doi:10.1016/j.jnucmat.2009.01.003

(Np,Pu)N [10–14]. Recently, (Np,Am)N, (Pu,Am)N, (Pu,Am,Cm)N and (Np,Pu,Am,Cm)N were successfully synthesized and analyzed [15].

The mixed nitrides of $(Np_{0.75}Am_{0.25})N$, $(Np_{0.50}Am_{0.50})N$, $(Np_{0.25}Am_{0.75})N$, $(Pu_{0.75}Am_{0.25})N$ and $(Pu_{0.50}Am_{0.50})N$ were prepared by the carbothermic reduction of mixtures of respective oxides in flowing N_2 gas at 1573–1773 K followed by heating in flowing N_2–4%H_2 mixed gas at 1773 K. The prepared nitrides were analyzed by X-ray diffraction and found to have a single phase of a NaCl-type structure to form the solid solution. The lattice parameters of the solid solutions of (Np,Am)N and (Pu,Am)N followed the Vegard's law in the NpN–AmN and PuN–AmN systems, respectively.

The X-ray diffraction analysis of $(Np_{0.279}Pu_{0.307}Am_{0.279}Cm_{0.135})N$ prepared by the carbothermic reduction method revealed the formation of a quaternary mononitride solid solution, as shown in Fig. 1. The lattice parameter of 0.4943 nm almost agreed with the value assumed from the Vegard's law. The present result experimentally confirmed the mutual miscibility among NpN, PuN, AmN and CmN. This property is favorable for the MA transmutation fuel, which could accommodate a wide range of the combination and composition of minor actinides.

2.2. Thermal expansions of actinide nitrides

The thermal expansions of NpN, PuN and AmN were determined from the temperature dependence of the lattice parameters measured by the high-temperature X-ray diffractometry [16]. The diffractometer installed in a glove box with a purified argon gas atmosphere was used to prevent the samples from hydrolysis and/or oxidation during handling and measurements. About 20 mg of the nitride powder prepared by the carbothermic reduction of the oxide was loaded on a platinum or tungsten holder. The measurements were carried out at room temperature to 1478 K.

The thermal expansions of NpN, PuN and AmN, together with that of the reported values for UN [17], are shown in Fig. 2. The thermal expansions of AmN and PuN were found to be close to each other and larger than that of UN, whereas the thermal expansion of NpN was nearly the same as that of UN.

The thermal expansion measurements on the single phase solid solution samples of $(Np_{0.55}Am_{0.45})N$, $(Pu_{0.59}Am_{0.41})N$, $(Np_{0.21}Pu_{0.52}Am_{0.22}Cm_{0.05})N$ and $(Zr_{0.61}Pu_{0.21}Am_{0.18})N$ were also carried out by the high-temperature X-ray diffraction technique at room temperature to 1478 K [18]. It was found that the average thermal expansion coefficient for each solid solution could be approximated from the values for the constituent nitrides by the linear mixture rule.

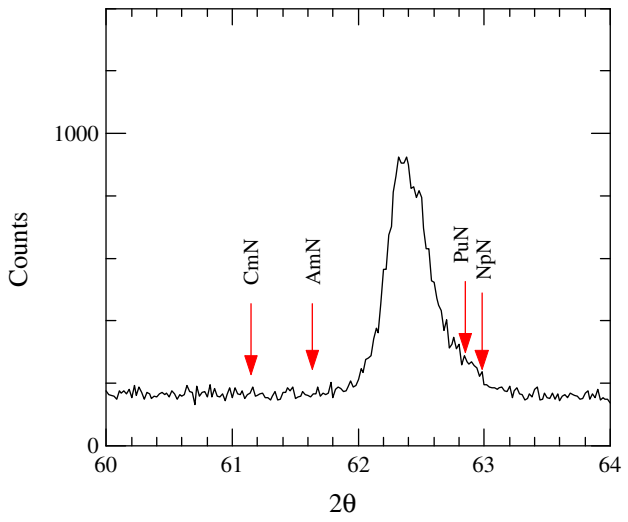

Fig. 1. X-ray diffraction pattern of $(Np_{0.279}Pu_{0.307}Am_{0.279}Cm_{0.135})N$ prepared by carbothermic reduction. Arrows indicate peak positions of respective mononitrides.

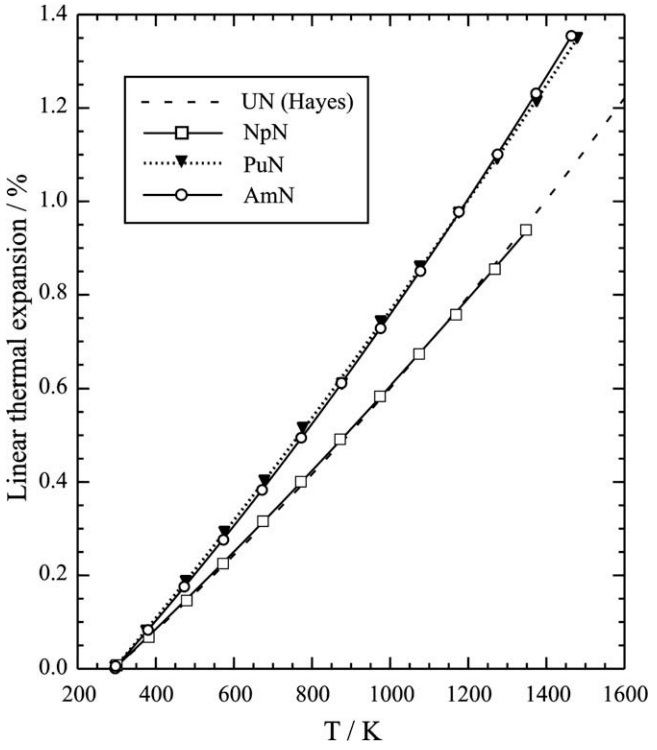

Fig. 2. Linear thermal expansions of NpN, PuN and AmN, together with that of UN [17], as a function of temperature.

2.3. Heat capacities of actinide nitrides

The heat capacities of NpN and AmN were determined by the drop calorimetry [19]. The NpN and AmN samples were prepared by the carbothermic reduction of the respective oxides. The enthalpy increments were measured with a twin-type drop calorimeter in a glove box. The apparatus consisted of two differential calorimetric units located in two cylindrical wells. The temperature difference between two calorimetric units was detected by Pt–Pt10%Rh thermocouples. The sample enclosed in a platinum container at room temperature was dropped into the calorimeter kept at a given temperature. The sapphire disk was used as standard. The heat capacities were determined by derivatives of the enthalpy increments.

The heat capacities of UN, PuN and NpN have been reported by Nakajima and Arai, where differential scanning calorimetry was used in the temperature range from 323 to 1023 K [20]. Their data on the heat capacities of UN and PuN agreed with the data in literature [21–23] within experimental errors and the heat capacity of NpN was nearly the same as those of UN and PuN.

The heat capacity of NpN obtained was in good agreement with the reported values [20]. The heat capacities of AmN and NpN obtained, together with those of UN [22] and PuN [23], are shown in Fig. 3. The heat capacity of AmN was found to be slightly smaller than those of UN, NpN and PuN.

The heat capacities of mixed actinide nitrides of (Np,Am)N, (Pu,Am)N, (Np,Pu,Am,Cm)N, (Pu,Am,Zr)N and (Np,Pu,Am,Cm,Zr)N are being studied by the drop calorimetry to test the validity of the Neumann–Kopp rule.

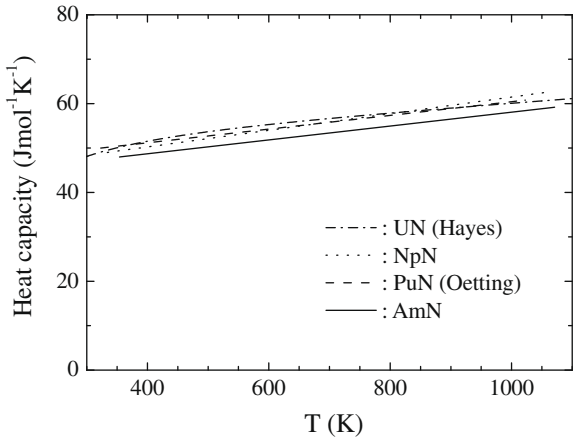

Fig. 3. Heat capacity of AmN, together with those of UN [22], NpN and PuN [23], as a function of temperature.

2.4. Thermal conductivities of actinide nitrides

The thermal diffusivity of AmN was measured by the laser-flash method at 373–1473 K [24]. The AmN powder prepared by the carbothermic reduction of the oxide was pressed into a disk followed by the sintering in flowing N_2–4%H_2 mixed gas at 1823 K for 10 h. The specimen used was about 3 mm in diameter and 0.6 mm in thickness. The apparatus has been installed in a glove box with a purified argon gas atmosphere. The data of temperature response curve at the rear surface of the specimen was analyzed by the curve fitting method. The thermal conductivity of AmN with the theoretical density was calculated with the measured thermal diffusivity, bulk density and specific heat capacity.

The thermal diffusivities of UN, NpN, PuN and the solid solutions of (U,Pu)N, (U,Np)N and (Np,Pu)N were previously measured by the laser-flash method from 740 to 1630 K, and the thermal conductivities have been reported as a function of temperature [25–27].

Fig. 4 shows the thermal conductivity of AmN, together with those of the reported values for UN, NpN and PuN [25,26]. The thermal conductivities of the actinide nitrides gradually increase with temperature over the temperature range investigated. For these nitrides, the electronic component contributes dominantly to the total thermal conductivity, and the increase in the thermal conductivity is due to the increase in the electronic component. It is also seen in Fig. 4 that the thermal conductivities decrease with increasing atomic number from UN to AmN. It is probable that the decrease is caused by the decrease in the electronic component contributing to the thermal conductivity. The electrical resistivity of actinide mononitride tends to increase with atomic number [27].

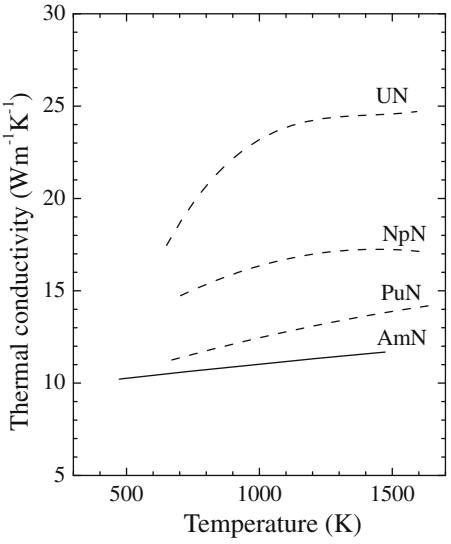

Fig. 4. Thermal conductivity of AmN, together with those of UN [25], NpN [26] and PuN [25], as a function of temperature.

The thermal diffusivity measurements of mixed actinide nitrides of (Np,Am)N, (Pu,Am)N, (Np,Pu,Am,Cm)N, (Pu,Am,Zr)N and (Np,Pu,Am,Cm,Zr)N are underway and the thermal conductivities are to be evaluated.

3. Properties of actinide oxides

3.1. Thermal expansions of actinide oxides

The thermal expansions of NpO_2, AmO_2 and Am_2O_3 were determined from the temperature dependence of the lattice parameters measured by the high-temperature X-ray diffractometry. The measurements were performed in flowing air for NpO_2 and AmO_2 and in flowing N_2–4%H_2 mixed gas for Am_2O_3.

The thermal expansions of UO_2, NpO_2, PuO_2, AmO_2 and CmO_2 were available in literature [28–31]. All the actinide dioxides have a face-centered cubic crystal structure. The thermal expansion of NpO_2 obtained was in good agreement with the reported values [29,30], and also that of AmO_2 agreed well with the reported values [30]. The crystal structure of Am_2O_3 is a hexagonal close-packed one. The thermal expansion of Am_2O_3 was not isotropic, where the thermal expansion along *c*-axis was larger than that along *a*-axis. The volume expansion of Am_2O_3 was about 1.14× as large as that of AmO_2.

The oxygen nonstoichiometry affects the thermal expansion and the control of the oxygen/metal ratio of the sample during measurement is important. The thermal expansion measurements by the high-temperature X-ray diffractometry on (Np,Am)O_2 and (Pu,Cm)O_2 are underway.

3.2. Heat capacities of actinide oxides

The heat capacity of NpO_2 was determined in the temperature range from 334 to 1071 K by the drop calorimetry [32]. A disk shaped NpO_2 sample was loaded in a platinum container, and then the container was evacuated and sealed in argon gas atmosphere. The enthalpy increment measurement was carried out with a twin-type drop calorimeter kept at a given temperature, in which the container at room temperature was dropped.

The heat capacity of NpO_2 obtained, together with those of the reported values for NpO_2 [33,34], UO_2 [35] and PuO_2 [35], are shown in Fig. 5. The present result of the heat capacity of NpO_2 at temperatures higher than 500 K was close to the values reported by Barin and Knacke [33], while it was smaller than the literature values [33,34] at temperatures lower than 500 K. The statistical error of the enthalpy increment in the present measurement was large below 500 K compared with that above 500 K, which may have caused the discrepancy. The heat capacity of NpO_2 determined in this study was slightly larger than that of UO_2 and about 7% smaller than that of PuO_2.

The heat capacities of AmO_2, Am_2O_3 and (Pu,Am)O_2 are being studied by the drop calorimetry.

3.3. Thermal conductivities of actinide oxides

The thermal diffusivities of AmO_{2-x} and NpO_2 were measured by the laser-flash method [32,36]. Disk samples of AmO_{2-x} and

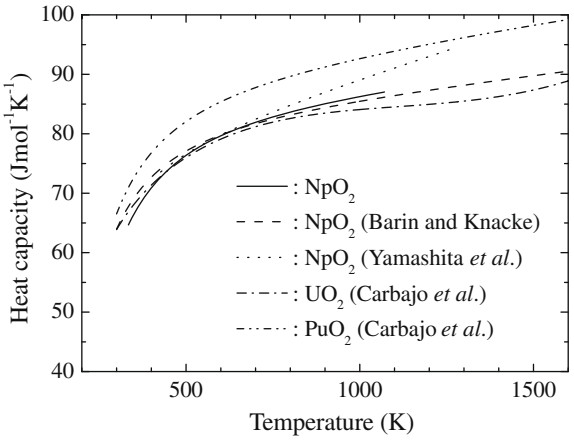

Fig. 5. Heat capacity of NpO_2, together with those of NpO_2 [33,34], UO_2 [35] and PuO_2 [35], as a function of temperature.

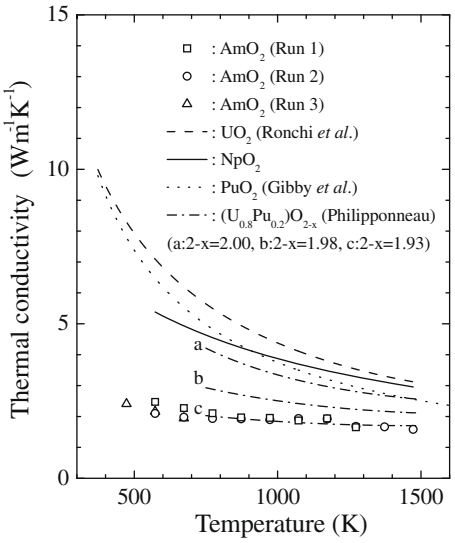

Fig. 6. Thermal conductivities of AmO_{2-x} and NpO_2, together with those of UO_2 [38], PuO_2 [39] and $(U_{0.8}Pu_{0.2})O_{2-x}$ [40], as a function of temperature.

NpO_2 were prepared by pressing and sintering the respective oxides in flowing air. The O/Am ratio of the disk could be about 1.9 at the beginning of the measurement. The thermal diffusivity measurements were performed in both the heating and cooling processes.

The thermal diffusivity of AmO_{2-x} at 573–773 K obtained in the first run was found to be larger than that in the second run, while the thermal diffusivity at 873–1273 K obtained in the first run was in good agreement with that in the second run. The data obtained in the third run were in good agreement with those in the second run. After the thermal diffusivity measurement, the O/Am ratio was found to be 1.73. In the case of a hypostoichiometric oxide, MO_{2-x}, it is known that the decrease in the O/M ratio results in the decrease in the thermal diffusivity. The thermal diffusivity of NpO_2 obtained in the heating and cooling measurements showed the good reproducibility.

The thermal conductivity of AmO_{2-x} with the theoretical density was calculated with the measured thermal diffusivity, bulk density and the specific heat capacity from literature [37], while the thermal conductivity of NpO_2 was calculated with the measured thermal diffusivity, bulk density and specific heat capacity.

The thermal conductivities of AmO_{2-x} and NpO_2, together with those of UO_2 [38], PuO_2 [39] and $(U_{0.8}Pu_{0.2})O_{2-x}$ [40] for comparison, are shown in Fig. 6. The thermal conductivity of AmO_{2-x} was smaller than those of the literature values of UO_2 and PuO_2. On the other hand, the thermal conductivity of NpO_2 from 873 to 1473 K lay between those of UO_2 and PuO_2. The thermal conductivities of AmO_{2-x} and NpO_2 decreased with increasing temperature in the temperature range investigated. This temperature dependence of the thermal conductivities of AmO_{2-x} and NpO_2 was similar to that of UO_2, PuO_2 and $(U_{0.8}Pu_{0.2})O_{2-x}$.

The thermal diffusivity measurements by the laser-flash method on $(Pu,Am)O_2$ and $(Np,Pu,Am)O_2$ are underway and the thermal conductivities are to be evaluated.

3.4. Oxygen potentials of actinide oxides

The oxygen potentials of AmO_{2-x} [41], $(Np,Am)O_{2-x}$ [42] and $(Pu,Am)O_{2-x}$ [43] were measured as a function of the oxygen nonstoichiometry x and temperature by the electromotive force method with a zirconia solid-electrolyte. For the measurements disks of the oxides with 3 mm in diameter and 1 mm in thickness were prepared. The galvanic cell type used was expressed by (Pt-electrode) sample/$Zr(Ca)O_{2-x}$/air (Pt-electrode).

Fig. 7 shows the oxygen potentials of AmO_{2-x} obtained as a function of the x at 1333 K, together with those of CeO_{2-x} at 988

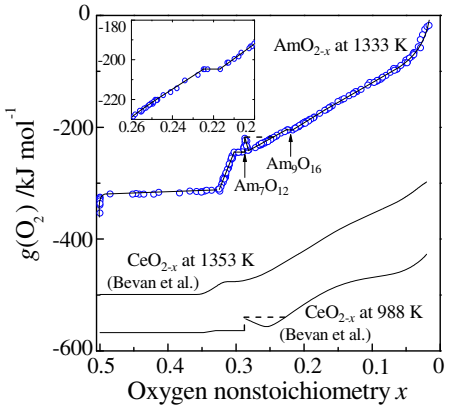

Fig. 7. Oxygen potentials of AmO_{2-x} at 1333 K, together with those of CeO_{2-x} at 1353 K and 988 K [44], as a function of the x.

and 1353 K [44] in literature. The relation between the oxygen potential and x of AmO_{2-x} is similar to those of CeO_{2-x}. The oxygen potentials of AmO_{2-x} changed from −20 to −360 kJ/mol with increasing x from 0.01 to 0.5 at 1333 K, which were higher than those of CeO_{2-x} at the corresponding x value by ~200 kJ/mol. The oxygen potentials obtained were almost consistent with the published phase diagram of the Am–O system. However, those suggested the presence of the intermediate stable phases of Am_9O_{16} and Am_7O_{12}.

Fig. 8 shows the oxygen potentials of $(Am_{0.5}Np_{0.5})O_{2-x}$ and AmO_{2-x} obtained as a function of the x at 1333 K, together with those of $(Am_{0.5}U_{0.5})O_{2-x}$ at 1333 K in literature [45]. The oxygen potentials of $(Am_{0.5}Np_{0.5})O_{2-x}$ suddenly dropped around −440 kJ/mol with increasing x. This could be attributed to the reduction of Am^{3+} to Am^{2+} or Np^{4+} to Np^{3+} at $x = 0.25$, where the chemical composition is $(Am^{3+}_{0.5}Np^{4+}_{0.5})O_{1.75}$. The oxygen potentials of $(Am_{0.5}Np_{0.5})O_{2-x}$ decreased smoothly from −93.63 to −440.1 kJ/mol with increasing x from 0.021 to 0.25. This result suggested that the $(Am_{0.5}Np_{0.5})O_{2-x}$ sample should be composed of the single oxygen-deficient fluorite-type phase in this x range at 1333 K. The oxygen potentials of $(Am_{0.5}Np_{0.5})O_{2-x}$ were higher than those of $(Am_{0.5}U_{0.5})O_{2-x}$ by ~200 kJ/mol at the corresponding x value.

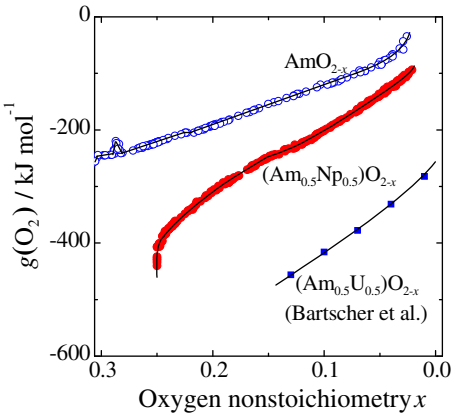

Fig. 8. Oxygen potentials of $(Am_{0.5}Np_{0.5})O_{2-x}$ at 1333 K, together with those of AmO_{2-x} at 1333 K and $(Am_{0.5}U_{0.5})O_{2-x}$ at 1333 K [45], as a function of the x.

For the oxygen potential measurements of $(Am_{0.5}Pu_{0.5})O_{2-x}$, the x was controlled at 1333 K over $0.02 < x \leqslant 0.25$ by the coulometric titration method. It was found that the oxygen potentials decreased smoothly with increasing x from 0.02 to 0.22 and that the oxygen potentials remained almost constant around $x = 0.23$. The tendency of the change in oxygen potential with increasing x from 0.02 to 0.22 at 1333 K for $(Am_{0.5}Pu_{0.5})O_{2-x}$ was similar to that for AmO_{2-x}. This suggested that the phase relations of $(Am_{0.5}Pu_{0.5})O_{2-x}$ should be similar to those of AmO_{2-x} at 1333 K over $0.02 < x \leqslant 0.25$.

4. Summary

The thermochemical and thermophysical properties of minor actinide nitrides and oxides, especially those of Am-bearing compounds, were studied and some measurements are underway. Table 1 summarizes the MA-bearing nitrides whose properties of thermal expansion, heat capacity and thermal conductivity are available in literature, reported in this paper and being studied by the authors. The properties of AmN were obtained and some Am-bearing mixed nitrides are being studied. However, the properties of CmN are still lacking though some data on Cm-bearing mixed nitrides are available. To clarify the effects of CmN on the properties of Cm-bearing mixed nitrides, the properties of CmN need to be obtained.

Table 1
MA-bearing nitrides whose properties are available in literature, reported in this paper and being studied by the authors.

Property	MA-bearing nitrides		
	In literature	Reported here	Being studied
Thermal expansion		NpN AmN (Np,Am)N (Pu,Am)N (Np,Pu,Am,Cm)N (Pu,Am,Zr)N	
Heat capacity	NpN	NpN AmN	(Np,Am)N (Pu,Am)N (Np,Pu,Am,Cm)N (Pu,Am,Zr)N (Np,Pu,Am,Cm,Zr)N
Thermal conductivity	NpN (U,Pu)N (U,Np)N (Np,Pu)N	AmN	(Np,Am)N (Pu,Am)N (Np,Pu,Am,Cm)N (Pu,Am,Zr)N (Np,Pu,Am,Cm,Zr)N

Table 2
MA-bearing oxides whose properties are available in literature, reported in this paper and being studied by the authors.

Property	MA-bearing oxides		
	In literature	Reported here	Being studied
Thermal expansion	NpO_2 AmO_2 CmO_2	NpO_2 AmO_2 Am_2O_3	$(Np,Am)O_2$ $(Pu,Cm)O_2$
Heat capacity	NpO_2	NpO_2	AmO_2 Am_2O_3 $(Pu,Am)O_2$
Thermal conductivity	$(U,Np)O_2$ $(U,Am)O_2$ $(U,Pu,Am)O_2$	NpO_2 AmO_2	$(Pu,Am)O_2$ $(Np,Pu,Am)O_2$
Oxygen potential	$(Th,Am)O_2$ $(U,Am)O_2$ $(Pu,Am)O_2$ $(U,Pu,Am)O_2$ $(U,Np,Pu,Am)O_2$	AmO_2 $(Np,Am)O_2$ $(Pu,Am)O_2$	

Table 2 summarizes the MA-bearing oxides whose properties of thermal expansion, heat capacity, thermal conductivity and oxygen potential are available in literature, reported in this paper and being studied by the authors. Like the situation of MA-bearing nitrides, the properties of americium oxides and some Am-bearing mixed oxides were obtained and are being studied, but the properties of curium oxides and Cm-bearing mixed oxides are still lacking.

Along with the property measurements, it is important to develop the modeling and simulation of the properties. The property measurements were carried out on single minor actinide compounds and then mixed ones to understand the effects of the mixture on the properties. With modeling and simulation, the properties of MA-bearing nitride and oxide fuels having any compositions would be estimated. This approach is especially favorable for the development of MA-bearing fuels since the experiments with MA will take a long time and cost a lot.

Acknowledgements

This paper contains some results obtained within the task 'Technological development of a nuclear fuel cycle based on nitride fuel and pyrochemical reprocessing' entrusted from the Ministry of Education, Culture, Sports, Science and Technology of Japan. This paper also contains some results obtained within the collaborative research program of TRU behavior in oxide fuels with Tohoku Electric Power Company, Tokyo Electric Power Company and the Japan Atomic Power Company.

References

[1] K. Minato, M. Akabori, M. Takano, Y. Arai, K. Nakajima, A. Itoh, T. Ogawa, J. Nucl. Mater. 320 (2003) 18.
[2] Y. Croixmarie, E. Abonneau, A. Fernandez, R.J.M. Konings, F. Desmoulière, L. Donnet, J. Nucl. Mater. 320 (2003) 11.
[3] A. Fernandez, D. Haas, J.P. Hiernaut, R.J.M. Konings, C. Nästren, H. Ottmar, D. Staicu, J. Somers, in: Proceedings of the Ninth OECD/NEA Information Exchange Meeting on Actinide and Fission Product Partitioning and Transmutation, 25–29 September, 2006, Nimes, France, 2007, p. 99.
[4] R. Thetford, M. Mignanelli, J. Nucl. Mater. 320 (2003) 44.
[5] K. Minato, M. Takano, T. Nishi, M. Akabori, Y. Arai, M. Uno, Adv. Sci. Technol. 45 (2006) 1931.
[6] M. Mignanelli, R. Thetford, in: Advanced Reactors with Innovative Fuels, OECD/NEA, 2001. p. 161.
[7] K. Minato, M. Akabori, T. Tsuboi, S. Kurobane, H. Hayashi, M. Takano, H. Otobe, M. Misumi, T. Sakamoto, I. Kato, T. Hida, Development of Module for TRU High Temperature Chemistry, Report JAERI-Tech 2005-059, 2005.
[8] M. Takano, A. Itoh, M. Akabori, T. Ogawa, S. Kikkawa, H. Okamoto, in: Proceedings of International Conference on Global '99, Jackson Hole, Wyoming, 29 August–3 September 1999, CD-ROM.

[9] M. Takano, A. Itoh, M. Akabori, T. Ogawa, M. Numata, H. Okamoto, J. Nucl. Mater. 294 (2001) 24.
[10] Y. Arai, S. Fukushima, K. Shiozawa, M. Handa, J. Nucl. Mater. 168 (1989) 280.
[11] Y. Suzuki, Y. Arai, Y. Okamoto, T. Ohmichi, J. Nucl. Sci. Technol. 31 (1994) 677.
[12] Y. Arai, Y. Suzuki, M. Handa, in: Proceedings of International Conference on Global '95, vol. 1, Versailles, France, 11–14 September 1995, p. 538.
[13] Y. Arai, T. Iwai, K. Nakajima, Y. Suzuki, in: Proceedings of International Conference on Global '97, vol. 1, Yokohama, Japan, 5–10 October 1997, p. 664.
[14] Y. Suzuki, T. Ogawa, Y. Arai, T. Mukaiyama, in: Proceedings of the Fifth OECD/NEA Information Exchange Meeting on Actinide and Fission Product Partitioning and Transmutation, 25–27 November, 1998, Mol, 1999, p. 213.
[15] Y. Arai, M. Akabori, K. Minato, in: Proceedings of International Conference on Global 2007, Boise, USA, 9–13 September 2007, p. 980.
[16] M. Takano, M. Akabori, Y. Arai, K. Minato, J. Nucl. Mater. 376 (2008) 114.
[17] S.L. Hayes, J.K. Thomas, K.L. Peddicord, J. Nucl. Mater. 171 (1990) 262.
[18] M. Takano, M. Akabori, Y. Arai, K. Minato, J. Nucl. Mater. 389 (2009) 89.
[19] T. Nishi, A. Itoh, M. Takano, M. Numata, M. Akabori, Y. Arai, K. Minato, J. Nucl. Mater. 377 (2008) 467.
[20] K. Nakajima, Y. Arai, J. Nucl. Sci. Technol. (Suppl. 3) (2002) 620.
[21] F.L. Oetting, J.M. Leitnaker, J. Chem. Thermodynam. 4 (1972) 199.
[22] S.L. Hayes, J.K. Thomas, K.L. Peddicord, J. Nucl. Mater. 171 (1990) 300.
[23] F.L. Oetting, J. Chem. Thermodynam. 10 (1978) 941.
[24] T. Nishi, M. Takano, A. Itoh, M. Akabori, K. Minato, M. Kizaki, J. Nucl. Mater. 355 (2006) 114.
[25] Y. Arai, Y. Suzuki, T. Iwai, T. Ohmichi, J. Nucl. Mater. 195 (1992) 37.
[26] Y. Arai, Y. Okamoto, Y. Suzuki, J. Nucl. Mater. 211 (1994) 248.
[27] Y. Arai, K. Nakajima, Y. Suzuki, J. Alloys Comp. 271–273 (1998) 602.
[28] Y.S. Touloukian (Ed.), Thermophysical Properties of Matter, vol. 13, IFI/Plenum, New York, 1977.
[29] T. Yamashita, N. Nitani, T. Tsuji, H. Inagaki, J. Nucl. Mater. 245 (1997) 72.
[30] J.A. Fahey, R.P. Turcotte, T.D. Chikalla, Inorg. Nucl. Chem. Lett. 10 (1974) 459.
[31] M. Noe, J.R. Peterson, Inorg. Nucl. Chem. Lett. 8 (1972) 897.
[32] T. Nishi, M. Takano, A. Itoh, M. Akabori, Y. Arai, K. Minato, M. Numata, J. Nucl. Mater. 376 (2008) 78.
[33] I. Barin, O. Knacke, Thermochemical Properties of Inorganic Substances, Springer, Berlin, Heidelberg, New York, 1973. p. 497.
[34] T. Yamashita, N. Nitani, T. Tsuji, T. Kato, J. Nucl. Mater. 247 (1997) 90.
[35] J.J. Carbajo, G.L. Yoder, S.G. Popov, V.K. Ivanov, J. Nucl. Mater. 299 (2001) 181.
[36] T. Nishi, M. Takano, A. Itoh, M. Akabori, Y. Arai, K. Minato, M. Numata, J. Nucl. Mater. 373 (2008) 295.
[37] R.J. Silva, G. Bidoglio, M.H. Rand, P.B. Robouch, H. Wanner, I. Puigdomenech, Chemical Thermodynamics of Americium, OECD/NEA, Elsevier, Amsterdam, 1995.
[38] C. Ronchi, M. Sheindlin, M. Musella, G.J. Hyland, J. Appl. Phys. 85 (1999) 776.
[39] R.L. Gibby, J. Nucl. Mater. 38 (1971) 163.
[40] Y. Philipponneau, J. Nucl. Mater. 188 (1992) 194.
[41] H. Otobe, M. Akabori, K. Minato, J. Am. Ceram. Soc. 91 (2008) 1981.
[42] H. Otobe, M. Akabori, Y. Arai, K. Minato, J. Am. Ceram. Soc. 92 (2009) 174.
[43] H. Otobe, M. Akabori, Y. Arai, J. Nucl. Mater. 389 (2009) 68.
[44] D.J.M. Bevan, J. Kordis, J. Inorg. Nucl. Chem. 26 (1964) 1509.
[45] W. Bartscher, C. Sari, J. Nucl. Mater. 118 (1983) 220.